A national laboratory of the U.S. Department of Energy
Office of Energy Efficiency & Renewable Energy

National Renewable Energy Laboratory
Innovation for Our Energy Future

Modal Dynamics of Large Wind Turbines with Different Support Structures

G. Bir and J. Jonkman
National Renewable Energy Laboratory

Presented at the ASME 27th International Conference on Offshore Mechanics and Arctic Engineering (OMAE2008)
Estoril, Portugal
June 15–20, 2008

Conference Paper
NREL/CP-500-43045
July 2008

NREL is operated by Midwest Research Institute ● Battelle Contract No. DE-AC36-99-GO10337

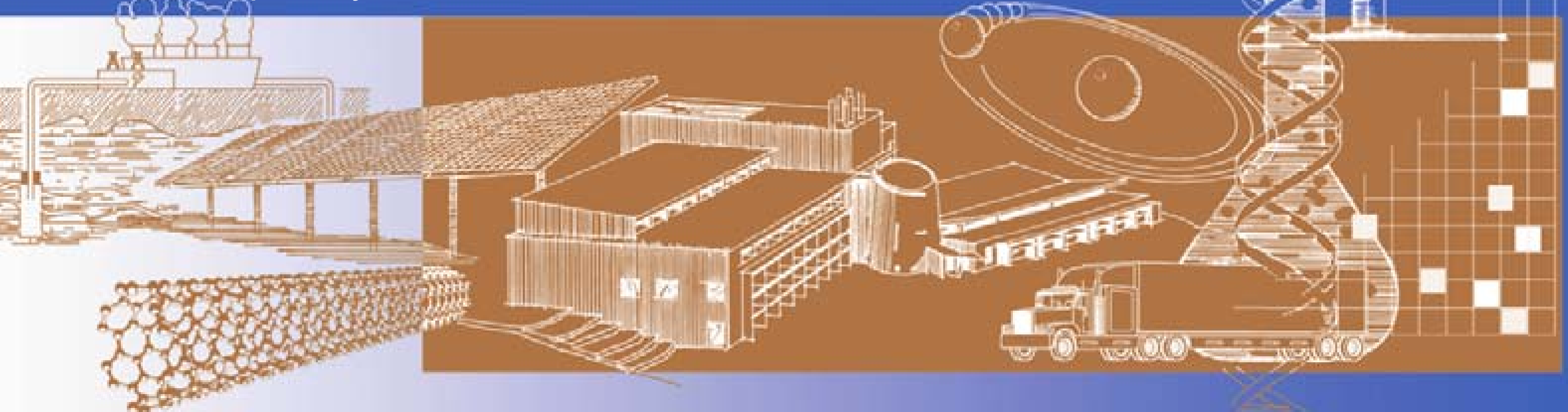

Available electronically at http://www.osti.gov/bridge

Available for a processing fee to U.S. Department of Energy
and its contractors, in paper, from:

U.S. Department of Energy
Office of Scientific and Technical Information
P.O. Box 62
Oak Ridge, TN 37831-0062
phone: 865.576.8401
fax: 865.576.5728
email: mailto:reports@adonis.osti.gov

Available for sale to the public, in paper, from:

U.S. Department of Commerce
National Technical Information Service
5285 Port Royal Road
Springfield, VA 22161
phone: 800.553.6847
fax: 703.605.6900
email: orders@ntis.fedworld.gov
online ordering: http://www.ntis.gov/ordering.htm

Printed on paper containing at least 50% wastepaper, including 20% postconsumer waste

MODAL DYNAMICS OF LARGE WIND TURBINES WITH DIFFERENT SUPPORT STRUCTURES*

Gunjit Bir **Jason Jonkman**
National Renewable Energy Laboratory
1617 Cole Blvd, Golden, Colorado, USA

ABSTRACT

This paper presents modal dynamics of floating-platform-supported and monopile-supported offshore turbines, which are gaining attention for their ability to capture the immense wind resources available over coastal waters. Minimal dynamic loads and the absence of instability are imperative to the success of these turbines. Modal dynamics determine both loads and instabilities to a large extent, and therefore must always be analyzed. Also, to model the turbine, several aeroelastic computer codes require modes of the major components, e.g., the rotor blades and the rotor-nacelle support structure. To compute such modes, we used a recently developed finite-element code called BModes. The code provides coupled modes either for the rotating blades or for the support structure. A coupled mode implies presence of coupled flexural, axial, and torsion motions in a natural mode of vibration. In this paper, we use BModes to provide modes only for flexible towers, which carry head mass (rotor-nacelle subassembly modeled as a rigid body) and are mounted atop either a floating platform or a soil-supported monopile. The code accounts for the effects of hydrodynamic inertia, hydrostatic restoring, and mooring lines stiffness on the floating platform. It also accounts for the distributed hydrodynamic mass on the submerged part of the tower and for the elastic foundation surrounding the monopile. Results are obtained for three turbine configurations: land-based turbine, floating-platform-supported turbine, and monopile-supported turbine. Three foundation models are used for the monopile configuration. Results show that the hydrodynamic and elastic-foundation effects strongly influence the turbine modal dynamics.

1. INTRODUCTION

Offshore wind turbines are gaining attention for their ability to capture the immense wind resources available over coastal waters. Monopile-supported turbines appear economical for shallow water; floating-platform-supported turbines may become so for deep water. Minimal dynamic loads and the absence of instability are imperative to the success of these turbines. The modal dynamics of a turbine determine both its loads and instabilities to a large extent. During the preliminary turbine design stages, designers examine modal characteristics to ensure that anticipated operational conditions will preclude resonances. During the refined design and analysis stages, analysts use modal dynamics to gain insight into dynamic couplings that determine loads, stability, and controls. Also, to model the wind turbine, several aeroelastic computer codes, e.g., FAST [1], require mode shapes of major turbine components, e.g., the rotor blades and the support structure. The fidelity of such mode shapes determines the fidelity of results obtained from these codes.

We had developed a finite-element code, called BModes (Beam Modal Analysis Code) [2], to determine high-fidelity modes of turbine blades, rotating or non-rotating, and land-based towers. Realizing the emerging interest in offshore turbines, we recently extended the code to also handle towers supported either on floating platforms or on monopile foundations. The code allows computation of coupled modes for both the blade and the tower support structure. A coupled mode implies presence of coupled flexural, axial, and torsion motions in a natural mode of vibration. Obtaining coupled modes accurately, particularly for a rotating blade, is one of the most challenging tasks in the dynamics field, and only a few codes address the issue. BModes uses a sophisticated finite-element approach in conjunction with analytical linearization and a special finite-element assembly that accurately captures Coriolis and centrifugal effects. The code relies on a 15-degree of freedom element with three internal and two boundary nodes. A salient feature of BModes is its potential to handle a complex range of boundary conditions.

The objective of this paper is to analyze modal characteristics of three wind turbine configurations: a land-supported turbine, a turbine mounted on top of a floating platform, and a turbine supported on a monopile foundation. Common to the three configurations is the baseline NREL 5-MW turbine [3], which is the rotor-nacelle part of the turbine mounted atop the support structure. Section 2 summarizes the baseline 5-MW turbine properties. We use BModes to determine modal characteristics of the three configurations, which differ only in the way the baseline turbine is supported.

Figure 1 shows the land-based configuration along with three offshore configurations, which have been considered as economical for different water depths [4]. For the land-based configuration, the support structure is simply a tower cantilevered to the ground. For the shallow-water configuration, the support structure is a tower mounted atop a monopile dug into the seabed. For the transitional-depth configuration, the support structure is a tower attached to a space frame, which can be a tripod (shown), a quadpod, or a lattice structure. For the deep-water configuration, the support structure is a tower mounted atop a floating platform, which is anchored to the seabed via tension cables (shown) or mooring lines. For the floating-platform-supported configuration, several concepts have been suggested in the literature. Of these concepts, three appear most promising: the Spar-Buoy concept, the Tension Leg Platform (TLP) concept, and the Barge concept. These differ in terms of the mechanism used to attain static stability. Refs 5-11 discuss modeling and engineering issues associated with these concepts.

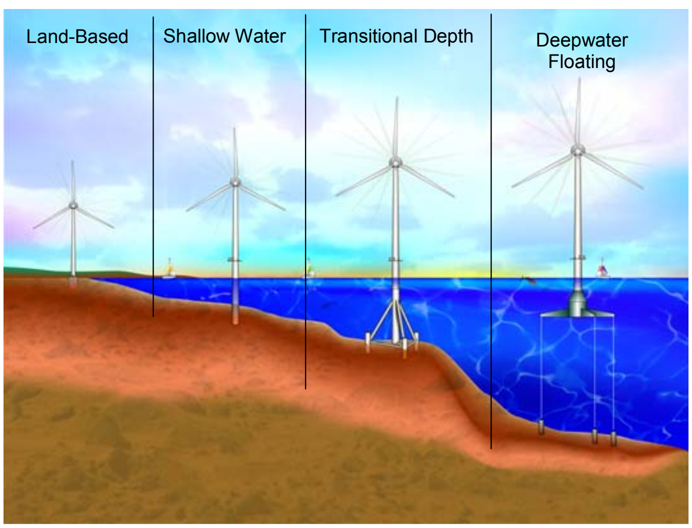

Figure 1. Floating wind turbine concepts.

BModes can handle all configurations except the transitional-depth configuration, which uses a space frame support structure. Using BModes, we analyze three configurations in this paper: a land-based turbine, a floating-platform-supported turbine, and a monopile-supported turbine. For the floating platform, we consider only the barge concept. Section 3 summarizes properties of this floating-platform configuration. Section 4 describes the monopile-supported configuration and the three models used to model this configuration.

Section 5 describes the modal analysis approach. In particular, it describes how we use BModes to develop a finite element model of a specific turbine configuration and obtain its modal characteristics. Section 6 discusses the modal results obtained for the three turbine configurations. For the floating-platform turbine, we study how the hydrodynamic-added mass and restoring alter the turbine modes. For the monopile-supported configuration, we compare modes resulting from the three models commonly used to model the monopile foundation. Section 7 summarizes conclusions and future work.

2. BASELINE TURBINE DESCRIPTION

The baseline turbine consists of an upwind, three-bladed, 126-meter diameter rotor mounted upwind on top of an 87.6-meter tower. Jonkman et al [3] established this concept so as to best match a few existing 5-MW designs. Salient turbine properties are summarized in Table 1; other properties can be found in the cited reference.

Table 1. Summary of Baseline Wind Turbine Properties.

Rating	5 MW
Rotor Orientation	Upwind
Rotor Diameter	126 m
Hub Height	90 m
Rotor Mass	110,000 kg
Nacelle Mass	240,000 kg
Tower Head c.m. offset in upwind direction	0.41 m
Tower Head c.m. vertical offset from tower top	1.97 m
Tower Head moment of inertia about rotor-parallel axis through c.m.	$4.37\text{X}10^7$ kg-m^2
Tower Head moment of inertia about lateral axis through c.m.	$2.35\text{X}10^7$ kg-m^2
Tower Head moment of inertia about vertical axis through c.m.	$2.54\text{X}10^7$ kg-m^2

Ref 3 provides the distributed mass, inertia, and stiffness properties of the tower. This NREL offshore 5-MW baseline wind turbine has been used to establish the reference specifications for a number of research projects supported by the U.S. Department of Energy's Wind Energy Technologies Program. In addition, the integrated European Union UpWind research program and the International Energy Agency Wind Annex XXIII Offshore Code Comparison Collaborative have adopted the NREL offshore 5-MW baseline wind turbine as their reference model.

3. FLOATING PLATFORM SUPPORT

In the floating-platform configuration, the 5-MW turbine described in the earlier subsection is mounted on top of a floating barge. We use a preliminary barge design developed by the Department of Naval Architecture and Marine Engineering at the Universities of Glasgow and Strathclyde under a contract with ITI Energy. The barge concept was chosen by ITI Energy because of its simplicity in design, fabrication, and installation. Not only is the barge designed to support a 5-MW baseline wind turbine, it also provides for an OWC (oscillating water column) wave power device, which is installed within a square moon pool located at the center of the barge and within the base of the wind turbine tower. We do not model the OWC assuming that its effect on turbine modal dynamics is negligible. The barge has a square section (40 x 40 m) and is ballasted with sea water. To prevent it from drifting, the platform is moored by a system of eight catenary lines, two of which emanate from each corner of the bottom of the barge, so that they are 45° apart at the corner. Table 2 lists salient features of the barge and mooring system. The concept is documented in greater detail in Ref 12.

Table 2. Summary of the ITI Energy Barge Properties**.**

Size (W×L×H)	40 m × 40 m × 10 m
Moon Pool (W×L×H)	10 m × 10 m × 10 m
Draft, Freeboard	4 m, 6 m
Water Displacement	6,000 m^3
Mass, Including Ballast	5,452,000 kg
Center of Mass (c.m.) below Mean Sea Level (MSL)	0.282 m
Roll Inertia about CM	726,900,000 kg·m^2
Pitch Inertia about CM	726,900,000 kg·m^2
Yaw Inertia about CM	1,453,900,000 kg·m^2
Anchor (Water) Depth	150 m
Separation Between Opposing Anchors	773.8 m
Unstretched Line Length	473.3 m
Neutral Line Length Resting on Seabed	250 m
Line Diameter	0.0809 m
Line Mass Density	130.4 kg/m
Line Extensional Stiffness	589,000,000 N

Figure 2 is a schematic of the floating-platform configuration analyzed in this paper.

4. MONOPILE-FOUNDATION SUPPORT

In the monopile-supported configuration, the turbine is installed on a monopile dug into the seabed (see leftmost schematic in Figure 3). The monopile foundation was designed by SWE (the Endowed Chair of Wind Energy at the University of Stuttgart in Germany) for the OC3 project [13-14]. As the figure shows, the flexible tower length is 143.6 m (comprising 87.6-m baseline-tower length, 20-m submerged tower length, and 36-m soil-supported tower length).

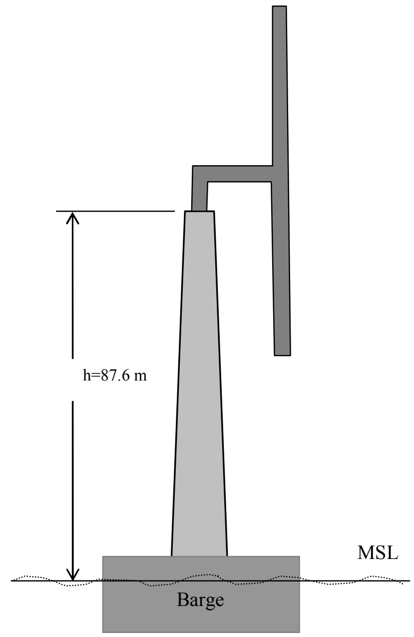

Figure 2. Floating-platform-supported turbine.

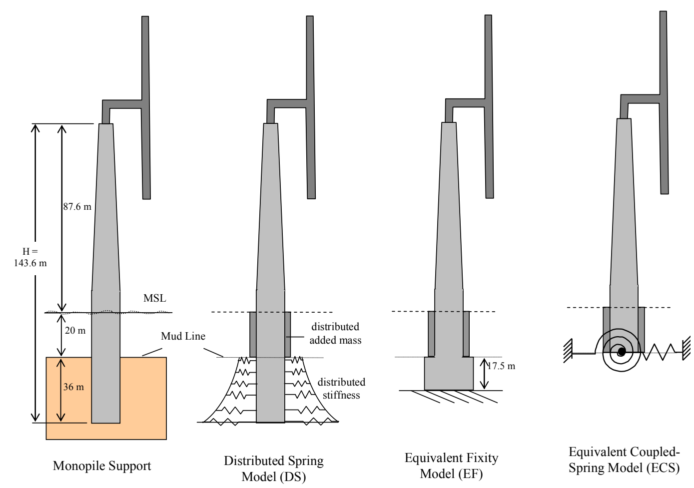

Figure 3. Monopile foundation and equivalent models.

The soil in reality behaves as a nonlinear elastic-plastic spring. However, most aeroelastic codes use a simpler representation. SWE derived three models to represent the monopile foundation (Figure 3): the distributed springs (DS) model, the coupled springs (CS) model, and the apparent fixity length (AF) model. In this paper, we designate the AF and CS models to be EF (equivalent fixity) and ECS (equivalent coupled springs) models, respectively.

The DS model idealizes the monopile with flexible foundation as a free-free beam with lateral (Winkler-type) springs distributed along the subsoil portion of the monopile. The beam uses the real properties of the monopile both above and below the mudline—including the real penetration depth. The subsoil spring stiffness constants are depth-dependent and are calculated using linearization of the lateral soil force versus lateral monopile displacement (*p-y*) data.

The EF model idealizes the monopile with flexible foundation as a cantilever beam whose properties are different above and below the mudline. The beam above the mudline has the real properties (i.e., diameter, thickness, and material) of the monopile. The beam below the mudline (17.5-m long tower part) has effective properties and a fictive length (i.e., the distance from the mudline to the cantilevered base) that are tuned so as to ensure that the overall response of the monopile above the mudline is the same as the response of the higher fidelity *p-y* model. The response can only be identical under a particular set of conditions, however, because the AF model is of lower fidelity. In the Offshore Code Comparison (OC3) project, the properties of the fictive beam were tuned such that the mudline displacement and rotation for both models would be the same when loaded by a mudline shear force and bending moment that are representative of the loading that exists when the offshore wind turbine is operating under normal conditions.

The ECS model idealizes the foundation compliance as a set of translational and rotational DOF (degrees of freedom) with coupled springs (i.e., a stiffness matrix) positioned at the mudline. Above the mudline, the monopile is modeled as a beam with the real properties of the monopile. The mudline spring stiffness constants were derived to give the same response as the EF model under the same loading conditions.

5. MODAL ANALYSIS APPROACH

To determine modal characteristics of each turbine configuration, we first develop its finite element model and obtain the associated global mass and stiffness matrices. Next, we perform eigenanalysis to obtain frequencies and mode shapes. We use BModes [2] for modeling a specific turbine configuration and for computing its modes. A brief description of BModes follows.

BModes provides dynamically-coupled modes for a beam. The beam can be a rotating or non-rotating rotor blade or a tower, and it can have arbitrary distribution of structural properties and geometry along its length. Both the blade and the tower can have end attachments. An end attachment is assumed to be a rigid body with mass, six moments of inertia, and a mass centroid that may be offset from the blade or tower axis. An example of an end attachment for a blade is the aerodynamic tip brake. For a tower, the end attachment can be a nacelle-rotor subassembly attached to the tower top. In addition to the tip inertia, the tower can also have tension-wire supports.

Recently, we extended BModes to model floating-platform and elastic foundation in conjunction with a mono-tower. The floating platform may be subjected to hydrodynamic-added mass, hydrostatic restoring, and mooring lines stiffness. These added mass and stiffnesses are generally distinct from physical inertias and springs and are expressed as 6X6 matrices associated with the six DOF (three translational and three rotational). For a monopile support, the soil effect is modeled as a distributed linear stiffness along the soil-buried part of the tower. Also, hydrodynamic-added mass may be specified along the submerged part of the tower (i.e., the part of the tower between the mean sea level (MSL) and the mudline).

As mentioned earlier, BModes provides coupled modes. A coupled mode implies presence of coupled flexural, axial, and torsion motions in a natural mode of vibration. Knowledge of coupled modes is crucial to several applications. Examples are: accurate modeling of major flexible components for modal-based aeroelastic codes such as FAST [1], validation of flexible component models using experimental data, modal-based fatigue analysis, and interpretation of aeroelastic-stability behavior of turbines.

Accurately obtaining rotating-blade or tower coupled modes is a challenging task, and only a few codes address the issue. BModes is perhaps the most accurate among these because it uses a finite-element approach in conjunction with analytical linearization and a special finite-element assembly that accurately captures Coriolis and centrifugal effects. Its finite-element approach, built on its predecessor UMARC [15], is based on a 15-degree-of-freedom element with three internal and two boundary nodes. The 15 DOF comprise 3 DOF for torsion deflection and 4 DOF each for axial, flap, and lag deflections (Figure 4). In the figure, u, v, w, and ϕ represent the axial, tower fore-aft, tower side-side, and twist DOF, respectively.

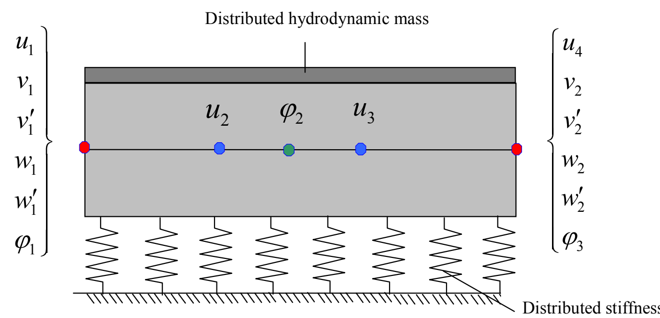

Figure 4. The 15-DOF finite element.

We recently upgraded the finite element to account for distributed stiffness and added mass, which may arise for platform- and monopile-supported towers. The added distributed hydrodynamic mass affects only the lateral displacements (*v, v', w, w'*) and not the torsion and axial motions. The distributed stiffness, like the distributed added mass, may vary along the element length and also may be different in the two lateral directions (normal to the element axis).

The BModes finite element approach allows for arbitrary variation of structural properties along each element of the beam. The structural properties are specified in terms of the tower fore-aft (F-A) bending stiffness, side-side (S-S) bending stiffness, axial stiffness; mass; section moments of inertia; and chordwise offsets of section shear center, tension center, and center-of-mass along the tower. The tower head (nacelle-rotor subsystem) and the tower base attachment (e.g., floating barge) are idealized as rigid bar elements.

A full discussion of the BModes theory basis is outside the scope of this paper. However, we provide an outline of the technical approach (Figure 5). First, we idealize the tower as an Euler-Bernoulli beam that undergoes F-A bending, S-S bending, elastic twist, and axial deflection. Next, we formulate energy expressions and use Hamilton's principle to derive coupled integro-partial differential equations (PDEs) governing the dynamics of elastic beam attached to rigid end inertias.

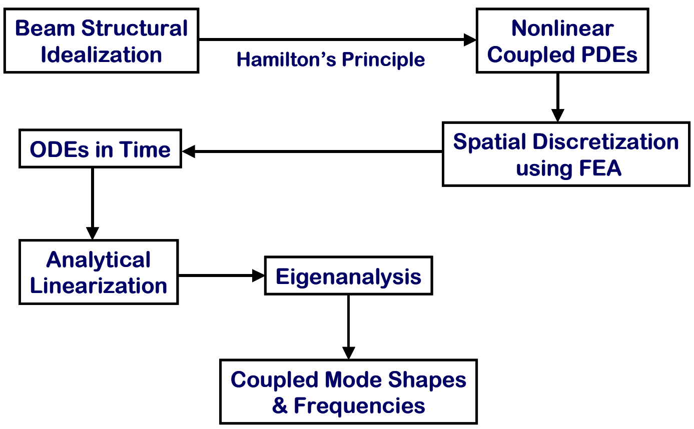

Figure 5. Technical approach: computation of tower coupled modes.

These PDEs are nonlinear and include spatial integral terms, which represent Coriolis and centrifugal effects. We use finite element analysis (FEA), the basis of modern structural analysis, to discretize the spatial (axial) variables in the PDEs. This FEA is compatible with Hamilton's principle. The beam is divided into a number of elements each with 15 DOF: Continuity of displacement and slope for F-A and S-S deflections and continuity of displacement for elastic twist and axial deflections are maintained between elements. The elastic twist is represented by a quasi-coordinate (non-Euler); this eliminates axial integral terms that otherwise would appear in orientation matrices for an elastic beam. Finite elements assembly, specialized for integro-partial differential equations, followed by application of appropriate boundary conditions, yields nonlinear ordinary differential equations (ODEs) in nodal coordinates. Analytical linearization (distinct from finite-differencing) yields inertia and stiffness matrices. We then perform an eigenanalysis to obtain the desired coupled modes and frequencies.

6. RESULTS

Before performing modal analyses on the platform-supported and monopile-supported wind turbines, we needed to verify BModes. The earlier version of BModes had been extensively verified using both analytical results and code-to-code comparison with the Rotorcraft Comprehensive Analysis System (RCAS) code developed by NASA [16]. Recent extensions to BModes necessitated further verification. We first used analytical models (e.g., uniform and tapered beams with end masses). Excellent agreement was obtained with all models. For a more realistic verification, we built several tower models using BModes and MSC.ADAMS (ADAMS). Results from select models will be presented where appropriate in the following subsections.

6.1. LAND-BASED TURBINE

Using BModes, we modeled the land-based tower as a beam cantilevered to the ground and computed its natural frequencies and mode shapes. Table 3 lists the modal frequencies of the tower (with and without the rotor-nacelle head mass) and also compares these with frequencies obtained from the ADAMS models. We used 50 finite elements in BModes and 99 tower parts in ADAMS. The head mass is idealized as a rigid mass and inertia in both BModes and ADAMS.

The modal frequencies are shown with four decimal points to aid verification. All frequencies, except very high ones, show good agreement. Also, for the tower without head mass, note that BModes predicts i^{th} F-A and i^{th} S-A modal frequencies to be identical as should be the case. Similar results from ADAMS differ, though by a very small margin. We believe BModes-computed results, particularly for higher modes, are more accurate, because it uses a consistent-mass approach, whereas ADAMS effectively uses a lumped mass approach, which is somewhat less accurate, to model the flexible tower. Note that the head mass substantially lowers all the modal frequencies. As mentioned earlier, the head mass (rotor-nacelle subsystem) is considered rigid. Flexibility of the rotor would somewhat alter the system frequencies and mode shapes; the torsion frequencies, in particular, would be much higher.

Figures 6 and 7 show the BModes-computed mode shapes for the land-based tower without and with the head mass (such modes are quantitatively difficult to extract from ADAMS, and this in fact motivated development of BModes). All mode shapes presented in this paper are mass-normalized. We do not normalize modes for unity tip deflection, as is typically done, for a reason we will explain shortly.

Without the head mass (figure 6), the tower fore-aft (F-A) and side-to-side (S-S) modes are identical as expected of an axi-symmetric tower.

The presence of the tower head mass introduces coupling between the side-to-side and torsion motions (Figure 7b). The fore-aft modes, however, remain uncoupled (Figure 7a). Also note that the head mass substantially alters the mode shapes. The rotary inertia of the head mass results in 2nd fore-aft and 2nd side-to-side mode shapes with near-zero deflections at the tower tip. An attempt to normalize such modes for unit tip deflections may lead to error-prone mode shapes. In fact, if the tip deflection were exactly zero (very possible in reality), it would be impossible to normalize modes for unity deflections. That is why BModes uses mass-normalization.

Table 3. Modal Frequencies of Land-Based Tower with and without Head Mass.

Mode Number	Mode Type	Without Head Mass Frequency (Hz)			With Head Mass Frequency(Hz)		
		BModes	ADAMS	Diff	BModes	ADAMS	Diff
1	1st SS	0.8913	0.8904	0.001	0.3291	0.3188	0.010
2	1st FA	0.8913	0.8904	0.001	0.3324	0.3218	0.011
3	2ndSS	4.3743	4.3437	0.031	1.8805	1.8820	0.002
4	2nd FA	4.3743	4.3435	0.031	2.2432	2.2391	0.004
5	3rd SS	11.3911	11.1856	0.205	4.6526	4.7244	0.072
6	3rd FA	11.3911	11.1843	0.207	4.9865	5.1833	0.197
7	1st Torsion	11.9656	11.4448	0.521	1.4703	1.4763	0.006
8	1st Axial	16.5217	16.5222	0.001	8.1311	7.9375	0.194
9	4th SS	21.8655	21.1146	0.751	11.3142	11.2678	0.046
10	4th FA	21.8655	21.1093	0.756	11.4591	11.4719	0.013
11	2nd Torsion	27.7783	26.1221	1.656	17.9632	17.9535	0.010
12	5th SS	35.8273	33.8392	1.988	21.7054	21.3291	0.376
13	5th FA	35.8273	33.8236	2.004	21.7625	21.4419	0.321
14	2nd Axial	43.4596	42.1715	1.288	30.2109	30.1182	0.093
15	3rd Torsion	44.8623	43.4578	1.405	35.3975	34.5078	0.890
16	6th SS	53.2770	48.9445	4.332	35.6336	34.5830	1.051
17	6th FA	53.2770	48.9071	4.370	35.6636	35.3740	0.290
18	4th Torsion	62.2312	58.6564	3.575	52.9449	50.5171	2.428
19	3rd Axial	71.4741	65.8776	5.596	53.0811	52.8981	0.183
20	7th SS	74.2155	65.9541	8.261	53.0673	50.5720	2.495

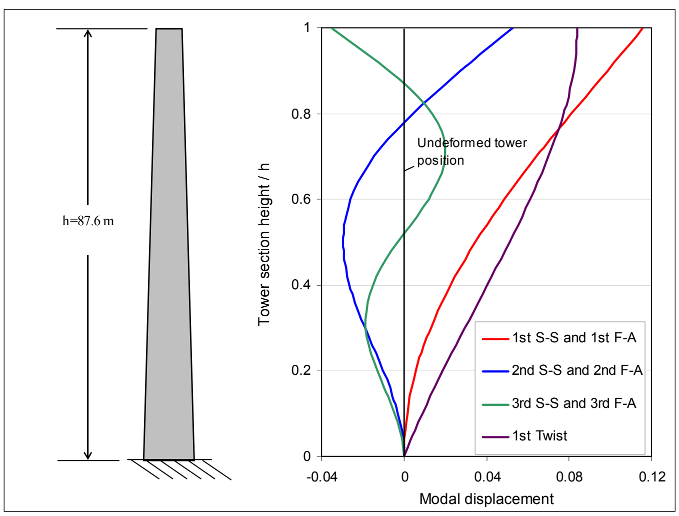

Figure 6. Modes of land-based tower without head mass.

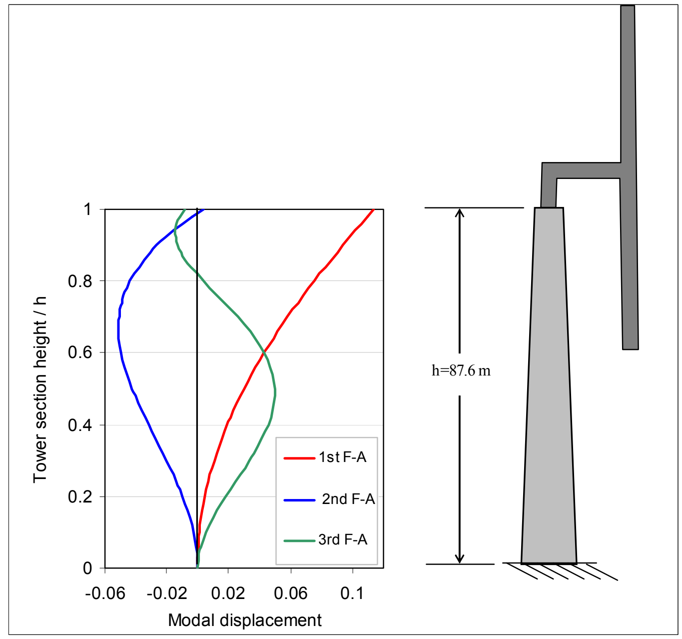

Figure 7a. Fore-aft modes of land-based tower with head mass.

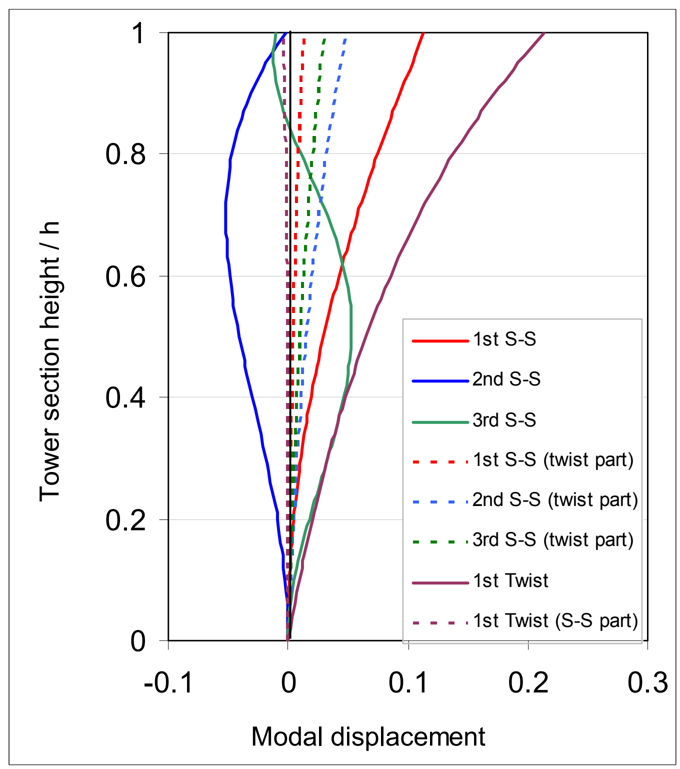

Figure 7b. Coupled side-to-side and twist modes for the land-based turbine.

6.2. FLOATING-PLATFORM-SUPPORTED TURBINE

Using BModes, we model the floating-platform-supported turbine as a beam with all the six DOF (three translational and three rotational) unconstrained at both ends. The tower-top end of the beam carries head mass and the tower-base end carries the platform modeled as a rigid body. To account for the hydrodynamic and hydrostatic effects on the platform, 6x6 inertia (added mass) and 6x6 restoring (stiffness) matrices, obtained from WAMIT [17], are input to BModes. The added mass values were chosen to be the values in the added mass matrix at the infinite-frequency limit of the frequency-dependent solution to the wave-radiation problem. A 6x6 matrix accounting for the mooring system stiffness is also included within BModes. This matrix was found by numerically linearizing the nonlinear mooring system module developed within FAST [1]. Because the particular configuration we select has no sea-submerged tower part, we do not include any distributed added mass (hydrodynamic) effect. Table 4 lists modal frequencies for three platform models: platform inertia only (platform physical inertia, but no added mass or stiffness), platform with all effects except the hydrodynamic added mass, and the full platform model.

In Table 4, the *surge* mode is the fore-aft motion of the platform. *Sway* is the side-to-side motion, *heave* is the up-down motion, *yaw* is the rotational motion about the tower axis, *roll* is the rotational motion about the platform longitudinal axis, and *pitch* is the rotational motion about the platform lateral axis. In the absence of any added mass and spring forces on the platform (platform-inertia-only model), the turbine behaves as a free-free flexible beam with two end inertias. Consequently, we observe six zero-frequency rigid-body modes. Note that the added hydrodynamic mass lowers all frequencies somewhat. The heave mode is lowered substantially (from 0.2576 Hz to 0.1283 Hz). The last column in the table lists ADAMS-computed frequencies for the full platform model. All frequencies agree well, except the heave frequency (identified in blue in the table). This result is because the ADAMS linearized model admits only a physical mass and inertia, whereas BModes permits the use of both physical and added masses. To account for the additional (hydrodynamic added) mass and inertia in the ADAMS model, we augmented the physical mass and inertia and altered the c.m. location of the barge. This could not be done perfectly because the actual hydrodynamic added mass of the barge in heave is quite different than the added mass in surge and sway (unlike the physical mass, which is identical in all directions). Our augmentation of the barge body mass properties ensured that the surge, sway, pitch, roll, and yaw elements (including off-diagonal elements)—but not the heave element—of the added mass matrix was accounted for in the ADAMS model.

Table 4. Modal Frequencies of Platform-Supported Turbine.

Mode Number	Mode Type	Frequency (Hz)			
		BModes			ADAMS
		Platform Inertia Only	Platform Inertia + Hydrostatic & Mooring Stiffness	Full Platform Model	Full Platform Model
1	Surge	0.0000	0.0081	0.0076	0.0076
2	Sway	0.0000	0.0081	0.0076	0.0076
3	Yaw	0.0000	0.0206	0.0198	0.0198
4	Roll	0.0000	0.1106	0.0978	0.0966
5	Pitch	0.0000	0.1109	0.0980	0.0968
6	Heave	0.0000	0.2576	0.1283	0.2463
7	1st SS	0.7349	0.7671	0.5489	0.5374
8	1st FA	0.7494	0.7820	0.5556	0.5440
9	1st Torsion	1.4836	1.4836	1.4826	1.4890
10	2nd SS	1.9943	1.9962	1.9270	1.9327
11	2nd FA	2.3652	2.3666	2.2942	2.2950
12	3rd SS	4.7559	4.7562	4.7011	4.7742
13	3rd FA	5.0799	5.0801	5.0293	5.2260
14	1st Axial	8.5014	8.5017	8.2186	8.2759
15	4th SS	11.3835	11.3835	11.3542	11.3138
16	4th FA	11.5280	11.5280	11.4983	11.5167
17	2nd Torsion	17.9683	17.9683	17.9679	17.9639
18	5th SS	21.7584	21.7584	21.7406	21.3760
19	5th FA	21.8153	21.8153	21.7975	21.4885
20	2^{nd} Axial	30.4368	30.4368	30.2625	30.3275

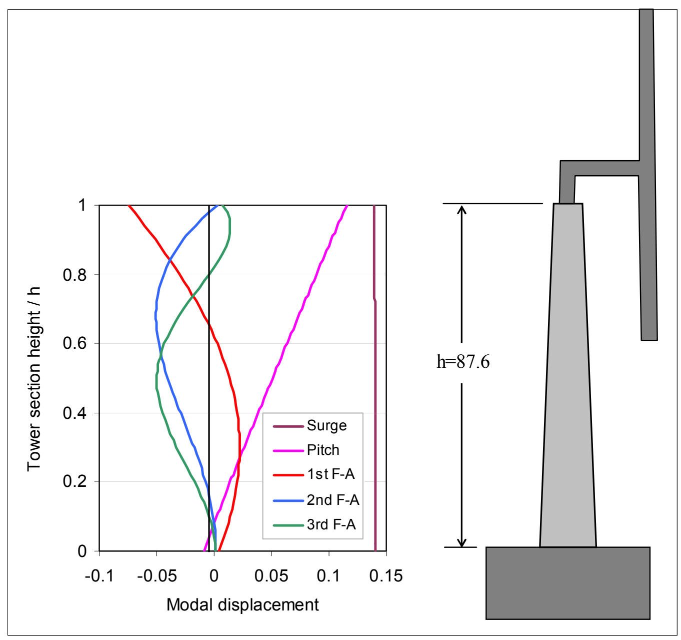

Figure 8a. Modes of platform-supported turbine.

Figures 8a–8c show BModes-computed mode shapes for the full platform-supported turbine model. Note that all modes in the longitudinal plane of symmetry of the turbine are uncoupled, whereas other modes are coupled. Note also that the low-frequency platform modes (surge, etc) are close to rigid-body modes as expected.

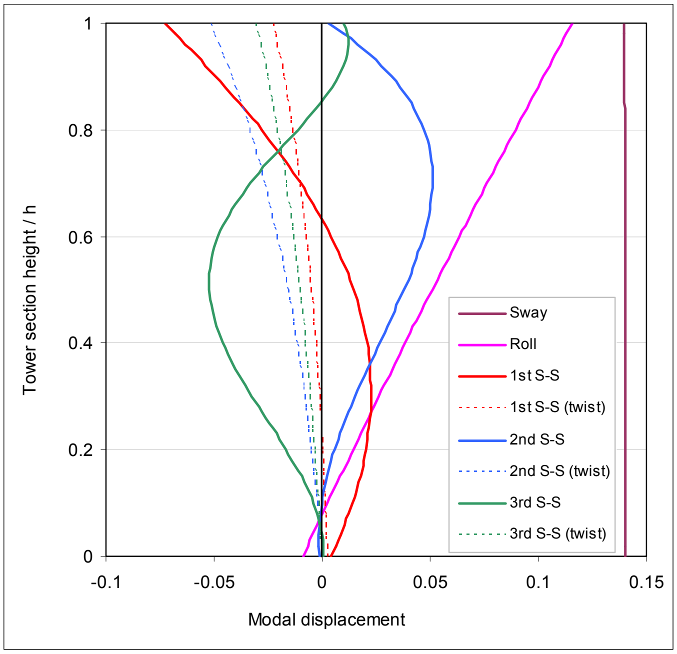

Figure 8b. Modes of platform-supported turbine.

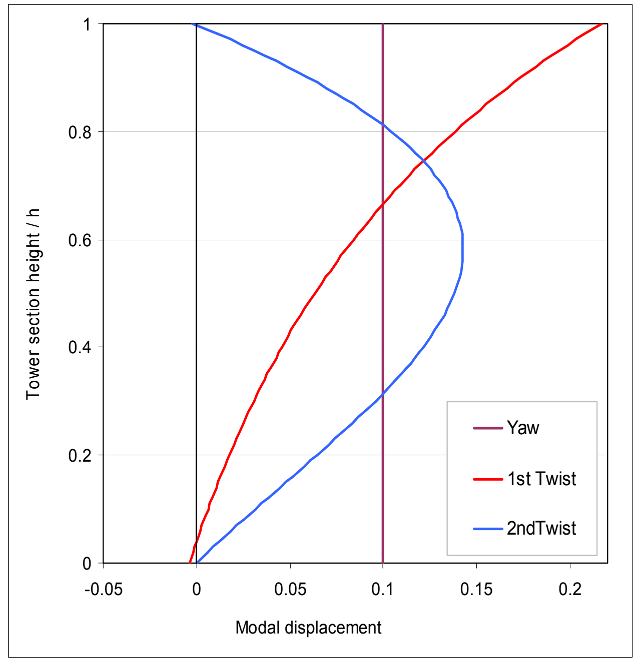

Figure 8c. Modes of platform-supported turbine.

6.3. MONOPILE-SUPPORTED TURBINE

As discussed in Section 4, three models have been proposed to represent the monopile foundation: the DS model, the EF model, and the ECS model. Figure 3 shows the three turbine configurations corresponding to these three models. We use BModes to model all these three models using the appropriate boundary conditions and the appropriate elastic foundation model. For the DS and ECS models, the axial and torsion motions were suppressed at the tower base.

Table 5 compares BModes- and ADAMS-computed modal frequencies for the DS model. All frequencies agree well, thereby verifying BModes modeling of the elastic foundation.

Table 6 compares modal frequencies obtained from the three monopile-supported turbine models. The DS model most closely represents the true monopile configuration and, therefore, must provide the most accurate frequencies and mode shapes. As seen in the table, the equivalent models (EF and ECS) provide reasonably accurate frequencies for the 1st fore-aft and 1st side-to-side modes. However, other frequencies differ appreciably. Results from the ECS model in particular diverge considerably because the ECS model, while partially accounting for the foundation stiffness, totally ignores the inertia of the tower foundation.

Figures 9a–9c compare BModes-computed mode shapes for the three monopile-supported turbine models. In these figures, which show tower modal deflection versus tower section height, the tower section height has been normalized with respect to *H*, the full height of the flexible tower, which is 143.6 m (see Figure 3). Thus, zero represents the flexible tower base and one represents the tower top. The figures also show the EF model fixity line, the mudline, and the MSL line locations on the tower axis. As seen in Figure 3, the flexible-tower base is located at one of these lines depending on which model we are considering. Mode shapes in Figures 9a–9c, which represent deflected shapes of only the flexible tower part of the turbine, originate at different reference lines. The reference line is the zero-tower-height line for the DS model, EF fixity line for the EF model, and mudline for the ECS model.

As the modal plots show, mode shapes of the three models agree reasonably for the 1st fore-aft, 1st side-to-side, and the 1st twist modes. Higher modes differ appreciably. This clearly implies that if higher modes participate in turbine dynamics, then equivalent EF and ECS models may lead to erroneous loads and stability predictions. The DS model would be the appropriate choice for such a case.

Table 5. Comparison of BModes- and ADAMS-Predicted Frequencies for the DS Model.

Mode Number	Mode Type	Frequency (Hz)		Difference (Hz)
		BModes	ADAMS	
1	1st SS	0.2513	0.2457	0.01
2	1st FA	0.2530	0.2472	0.01
3	1st Torsion	1.2752	1.2777	0.00
4	2nd SS	1.3680	1.3549	0.01
5	2nd FA	1.5316	1.5056	0.03
6	3rd SS	2.7425	2.7810	0.04
7	3rd FA	3.0874	3.1788	0.09
8	4th SS	5.9778	6.0090	0.03
9	4th FA	6.0506	6.2269	0.18
10	1st Axial	6.7671	6.5515	0.22
11	2nd Torsion	10.3875	10.3448	0.04
12	5th SS	11.4049	11.2947	0.11
13	5th FA	11.4758	11.4022	0.07
14	6^{th} SS	17.9595	17.6518	0.31
15	6^{th} FA	17.9704	17.7208	0.25
16	2^{nd} Axial	18.1887	18.0404	0.15
17	3^{rd} Torsion	21.1075	21.1944	0.09
18	7^{th} SS	26.3980	25.7959	0.60
19	7^{th} FA	26.4215	25.8452	0.58
20	4^{th} Torsion	32.9711	32.8559	0.12

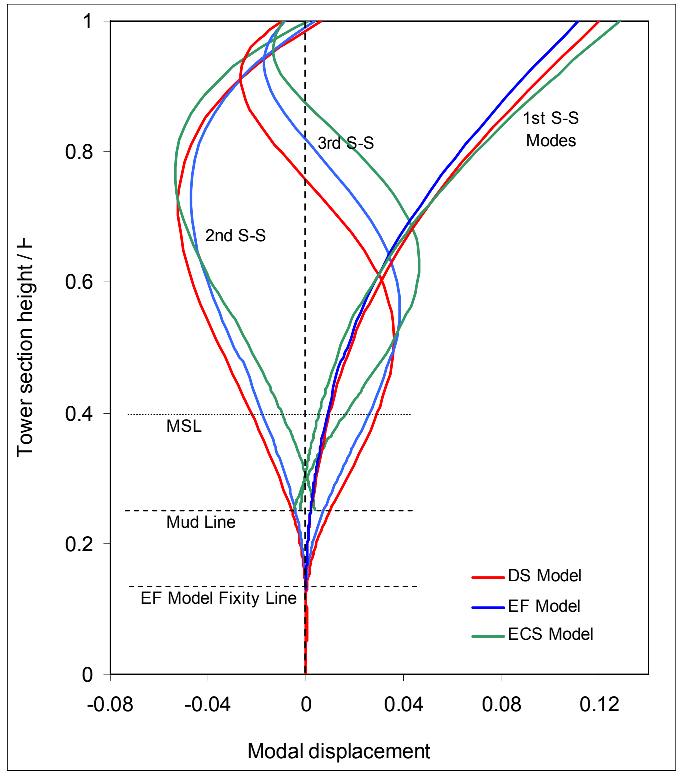

Figure 9a. Side-to-side modes of monopile-supported turbine models.

Table 6. Comparison of Modal Frequencies for the DS, EF, and ECS Turbine Models.

Mode Number	Mode Type	Frequency (Hz)		
		Distributed Stiffness	Apparent Fixity	Equivalent Stiffness
1	1st SS	0.2513	0.2513	0.2584
2	1st FA	0.253	0.2530	0.2604
3	1st Torsion	1.2752	1.3039	1.3223
4	2nd SS	1.368	1.3672	1.5051
5	2nd FA	1.5316	1.5307	1.7468
6	3rd SS	2.7425	2.7430	3.3313
7	3rd FA	3.0874	3.0895	3.6600
8	4th SS	5.9778	6.0125	7.1579
9	4th FA	6.0506	6.1083	7.6287
10	1st Axial	6.7671	7.0695	7.8420
11	2nd Torsion	10.3875	11.6387	13.1516
12	5th SS	11.4049	11.7126	13.1865
13	5th FA	11.4758	13.1636	15.9651
14	6^{th} SS	17.9595	18.7032	16.6629
15	6^{th} FA	17.9704	18.7399	16.6988
16	2^{nd} Axial	18.1887	22.2298	25.9700
17	3^{rd} Torsion	21.1075	23.3796	25.9937
18	7^{th} SS	26.398	28.0710	26.8848
19	7^{th} FA	26.4215	28.0961	28.2832
20	4^{th} Torsion	32.9711	38.1141	38.7023

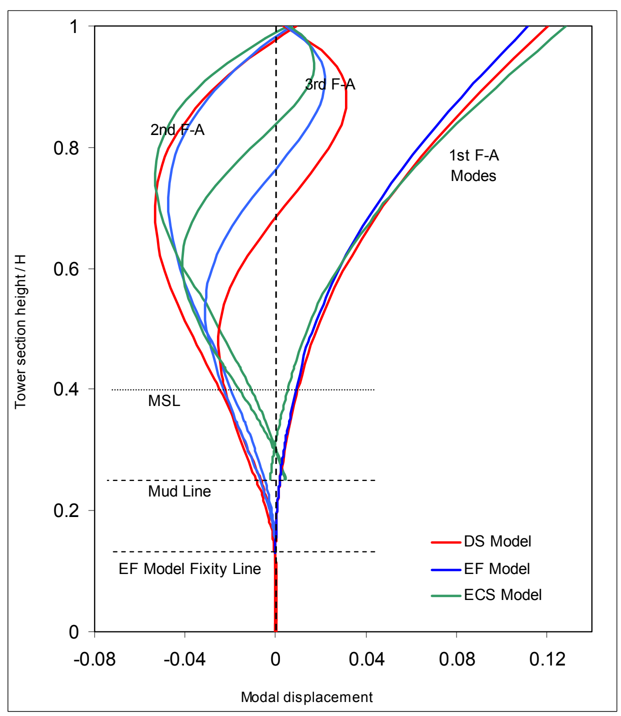

Figure 9b. Fore-aft modes of monopile-supported turbine models.

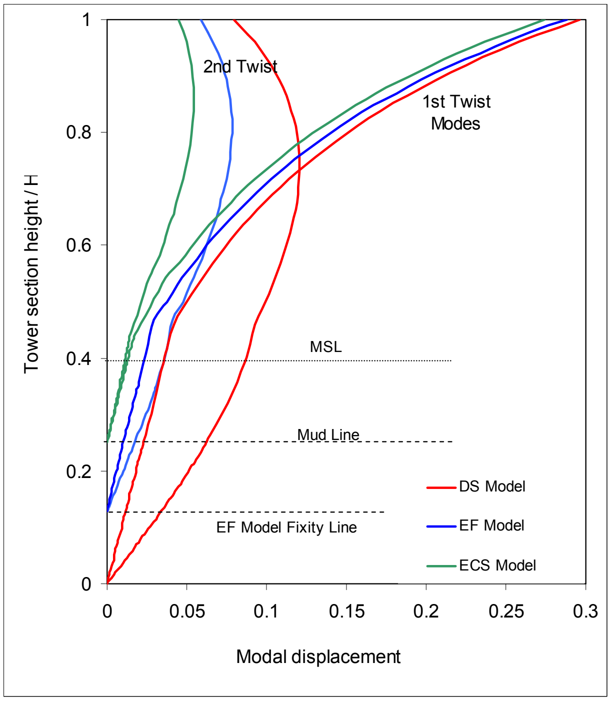

Figure 9c. Torsion modes of monopile-supported turbine models.

7. CONCLUSIONS

We successfully used BModes, a finite element code upgraded recently, to compute modal characteristics of three turbine configurations: a land-based turbine, a floating-platform-supported offshore turbine, and a monopile-supported offshore turbine. Results show that hydrodynamic effects for the floating-platform-supported turbine and elastic foundation effects for the monopile-supported turbine have substantial influence on the turbine modes. For the monopile-supported turbine, we considered three models proposed in the literature: the DS model, the EF model, and the ECS model. Results suggest that if higher modes play a role in turbine dynamics under certain operating conditions, then the equivalent EF and ECS models may lead to erroneous loads and stability predictions. The DS model would be the appropriate choice for such cases.

In the near future, we plan to write user's manual for the recently upgraded BModes and then post the manual and the code on the NREL website.

ACKNOWLEDGMENTS

Thanks to Sandy Butterfield for motivating the development of BModes, and to Marshall Buhl for his software-related support. DOE supported this work under contract number DE-AC36-83CH10093.

REFERENCES

1. Jonkman, J.M.; Buhl Jr., M.L. *FAST User's Guide*. NREL/EL-500-29798. Golden, Colorado: National Renewable Energy Laboratory, 2005.
2. Bir, G.S. *User's Guide to BModes: Software for Computing Rotating Beam Coupled Modes*. NREL TP-500-38976. Golden, Colorado: National Renewable Energy Laboratory, 2005.
3. Jonkman, J.; Butterfield, S.; Musial, W.; and Scott, G. *Definition of a 5-MW Reference Wind Turbine for Offshore System Development*. NREL/TP-500-38060. Golden, CO: National Renewable Energy Laboratory, February 2007.
4. Musial, W. and Butterfield, S. "Future for Offshore Wind Energy in the United States." *EnergyOcean Proceedings; June 2004, Palm Beach, Florida, USA. CP-500-36313.* Golden, CO: National Renewable Energy Laboratory, 2004.
5. Butterfield, Sandy; Musial, Walt; Jonkman, Jason; Sclavounos, Paul; and Wayman, Libby. "Engineering Challenges for Floating Offshore Wind Turbines." *Copenhagen Offshore Wind 2005 Conference and Expedition Proceedings, 26–28 October 2005.* Copenhagen, Denmark: Danish Wind Energy Association, October 2005.
6. Lee, Kwang Hyun. *Responses of Floating Wind Turbines to Wind and Wave Excitation*. M.S. Dissertation. Cambridge, Massachusetts: Department of Ocean Engineering, Massachusetts Institute of Technology, January 2005.
7. Wayman, E. N.; Sclavounos, P. D.; Butterfield, S.; Jonkman, J.; and Musial, W. "Coupled Dynamic Modeling of Floating Wind Turbine Systems." *2006 Offshore Technology Conference Proceedings, 1-4 May 2006, Houston, TX*, NREL/CP-500-39481. Richardson, TX: Offshore Technology Conference, May 2006, OTC 18287.
8. Wayman, Elizabeth. *Coupled Dynamics and Economic Analysis of Floating Wind Turbine Systems*. M.S. Dissertation. Cambridge, Massachusetts: Department of Mechanical Engineering, Massachusetts Institute of Technology, June 2006.
9. Henderson, Andrew R. and Patel, Minoo H. "On the Modelling of a Floating Offshore Wind Turbine." *Wind Energy*, Vol. 6, No. 1, February 2003; pp. 53–86.
10. Withee, John E. *Fully Coupled Dynamic Analysis of a Floating Wind Turbine System*. Ph.D. Dissertation. Cambridge, Massachusetts: Department of Ocean Engineering, Massachusetts Institute of Technology, 2004.
11. Jonkman, J.M. *Dynamics Modeling and Loads Analysis of an Offshore Floating Wind Turbine.* Ph.D. Thesis. Boulder, CO: Department of Aerospace Engineering Sciences, University of Colorado, 2007; National Renewable Energy

Laboratory/TP-500-41958, Golden, CO: National Renewable Energy Laboratory.

12. Vijfhuizen, W. J. M. J. *Design of a Wind and Wave Power Barge*. M.S. Dissertation. Glasgow, Scotland: Department of Naval Architecture and Mechanical Engineering, Universities of Glasgow and Strathclyde, September 2006.

13. Passon, P. "Memorandum: Derivation and Description of the Soil-Pile-Interaction Models." Endowed Chair of Wind Energy, University of Stuttgart, Stuttgart, Germany, 2006 (unpublished).

14. Jonkman, J.; Butterfield, S.; Passon, P.; Larsen, T.; Camp, T.; Nichols, J.; Azcona, J.; and Martinez, A. "Offshore Code Comparison Collaboration within IEA Wind Annex XXIII: Phase II Results Regarding Monopile Foundation Modeling." NREL/CP-500-42471. Golden, CO: National Renewable Energy Laboratory, 2008.

15. Bir, G. S., and Chopra, I. "Status of the University of Maryland Advanced Rotorcraft Code (UMARC)." *Presented at the American Helicopter Society Aeromechanics Specialist Conference.* San Francisco, California, January 19-21, 1994.

16. Bir, G. S.. Structural Dynamics Verification of Rotorcraft Comprehensive Analysis System (RCAS). NREL/TP-500-35328. Golden, CO: National Renewable Energy Laboratory, 2005.

17. Lee, C. H. and Newman, J. N. WAMIT® User Manual, Versions 6.3, 6.3PC, 6.3S, 6.3S-PC. Chestnut Hill, MA: WAMIT, Inc., 2006.

REPORT DOCUMENTATION PAGE

Form Approved
OMB No. 0704-0188

1. REPORT DATE *(DD-MM-YYYY)* July 2008	**2. REPORT TYPE** Conference paper	**3. DATES COVERED** *(From - To)* June 15 - 20, 2008

4. TITLE AND SUBTITLE Modal Dynamics of Large Wind Turbines with Different Support Structures	**5a. CONTRACT NUMBER** DE-AC36-99-GO10337
	5b. GRANT NUMBER
	5c. PROGRAM ELEMENT NUMBER
6. AUTHOR(S) G. Bir and J. Jonkman	**5d. PROJECT NUMBER** NREL/CP-500-43045
	5e. TASK NUMBER WER8.2006
	5f. WORK UNIT NUMBER

7. PERFORMING ORGANIZATION NAME(S) AND ADDRESS(ES) National Renewable Energy Laboratory 1617 Cole Blvd. Golden, CO 80401-3393	**8. PERFORMING ORGANIZATION REPORT NUMBER** NREL/CP-500-43045
9. SPONSORING/MONITORING AGENCY NAME(S) AND ADDRESS(ES)	**10. SPONSOR/MONITOR'S ACRONYM(S)** NREL
	11. SPONSORING/MONITORING AGENCY REPORT NUMBER

12. DISTRIBUTION AVAILABILITY STATEMENT
National Technical Information Service
U.S. Department of Commerce
5285 Port Royal Road
Springfield, VA 22161

13. SUPPLEMENTARY NOTES

14. ABSTRACT *(Maximum 200 Words)*

This paper presents modal dynamics of floating-platform-supported and monopile-supported offshore wind turbines.

15. SUBJECT TERMS
offshore wind turbines; wind turbine design; wind turbine modeling; wind energy.

16. SECURITY CLASSIFICATION OF:			**17. LIMITATION OF ABSTRACT**	**18. NUMBER OF PAGES**	**19a. NAME OF RESPONSIBLE PERSON**
a. REPORT	**b. ABSTRACT**	**c. THIS PAGE**			
Unclassified	Unclassified	Unclassified	UL		**19b. TELEPHONE NUMBER** *(Include area code)*

Standard Form 298 (Rev. 8/98)
Prescribed by ANSI Std. Z39.18